

We are IntechOpen, the world's leading publisher of Open Access books Built by scientists, for scientists

5,500

Open access books available

136,000

International authors and editors

170M

Downloads

Our authors are among the

154

Countries delivered to

TOP 1%

most cited scientists

12.2%

Contributors from top 500 universities



WEB OF SCIENCE™

Selection of our books indexed in the Book Citation Index
in Web of Science™ Core Collection (BKCI)

Interested in publishing with us?
Contact book.department@intechopen.com

Numbers displayed above are based on latest data collected.
For more information visit www.intechopen.com



One-Dimensional Modeling of Triple-Pass Concentric Tube Heat Exchanger in the Parabolic Trough Solar Air Collector

Nguyen Minh Phu and Ngo Thien Tu

Abstract

The parabolic trough solar collector has a very high absorber tube temperature due to the concentration of solar radiation. The high temperature leads to large heat loss to the environment which reduces efficiency of the parabolic trough collector. The heat loss reduction can be obtained by adopting a multi-pass fluid flow arrangement. In this chapter, airflow travels in three passes of the receiver to absorb heat from the glass covers and absorber tube to decrease surface temperatures. 1D mathematical model is developed to evaluate effective efficiency and the temperature distribution of surfaces and fluid. The mathematical modeling is based on air temperature gradients and solved by a numerical integration. Diameter ratios of outer glass to inner glass (r_{23}) and inner glass to absorber tube (r_{12}), Reynolds number (Re), and tube length (L) are varied to examine the efficiency and the temperature distribution. Results showed that the highest efficiency is archived at $r_{23} = 1.55$ and r_{12} in the range of 1.45 to 1.5. The efficiency increases with Re and decreases with L due to dominant heat transfer in terms of thermohydraulic behavior of a concentrating solar collector. With the optimum ratios, absorber tube temperature can reduce 15 K compared with another case.

Keywords: Concentric tube heat exchanger, 1D modeling, parabolic trough collector, effective efficiency, solar air heater

1. Introduction

Today, energy saving is a matter of great concern due to the depletion of fossil fuels as well as environmental pollution. Faced with that situation, the problem is that we must take advantage of available energy sources and use them for a long time without emitting toxic substances that affect the current living environment. Solar energy is a very abundant, completely free, environmentally friendly and long-lasting source of energy. Besides, it is possible to reduce the amount of toxic waste into the environment and contribute to saving a significant amount of costs when perceiving how to apply solar energy in daily life. Producing hot air by solar energy is an efficient and green solution by using a solar air heater. Flat-plate solar collector is often used in the range of moderately hot air temperature [1–3]. To generate greater air temperature, concentrating solar collectors are used. There are several types of concentrating collector such as linear Fresnel collector, dish

collector, and parabolic trough collector. The parabolic trough collector is attributed to the most widespread one [4]. Sketch and pictorial view of a parabolic trough solar collector are shown in **Figures 1** and **2**. When the intensity of solar radiation reaches the parabolic surface, solar energy is reflected and concentrated into the focus of the parabola where locates a thermal receiver. Here the heating process takes place to heat up a heat transfer fluid inside the receiver.

Elakhdar et al. [4] used a parabolic trough collector to power the generator of an organic Rankine plant. The results shown that the heat transfer fluid temperature in the receiver tube is up to 430 K and the thermal efficiency of the plant is 0.14. Li and Yuan [5] employed a parabolic trough collector for lighting and heating purposes. The results were reported that the lighting efficiency reaches 16.3%, the thermal efficiency 23.1% and the payback period less than 10 years. Bozorg et al. [6] numerically investigated a parabolic trough collector with nanofluid as a heat transfer media. It is proved that heat transfer, pressure drop, and thermal efficiency increase linearly with Reynolds number. Bellos et al. [7] examined a parabolic

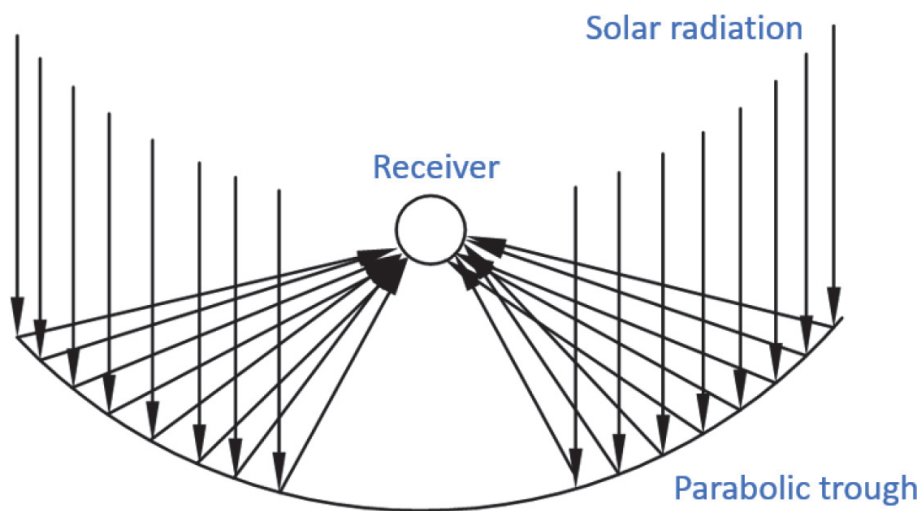


Figure 1.
Parabolic trough solar collector.



Figure 2.
The parabolic trough solar collector being tested at the Ho Chi Minh City University of Technology.

trough collector for thermal energy storage. The thermal efficiency and exergy efficiency of their system indicated 68.7% and 8.5%, respectively. Higher storage tank volume is recommended to yield higher thermal efficiency. Okonkwo et al. [8] studied different configurations of absorber tube including smooth tube, finned tube, twisted tape inserted tube, and converging–diverging tube. The results exhibited that the converging–diverging absorber tube demonstrated the highest exergy efficiency. In addition, the optical losses are the main components of exergy losses. Kaloudis et al. [9] simulated the absorber tube with an inner solid plug as a flow restriction device. In the study, the heat transfer fluid of Al₂O₃ nanofluid 4% revealed the best collector efficiency. Ray et al. [10] conducted a numerical analysis of selective coatings on the absorber tube. The thermal efficiency can be increased up to 34.6% by the selective coating. Tzivanidis and Bellos [11] used a parabolic trough collector to drive an absorption chiller which is to cool a room. The size of collector and thermal storage tank were determined to meet cooling load of a given space. Ghasemi and Ranjbar [12] compared heat transfer fluids of water and nanofluid inside a absorber tube. They confirmed that the nanofluid can improve heat transfer rate compared with the water. Nain et al. [13] employed the U-tube in a parabolic trough air collector. The tube was covered by the evacuated glass tube to minimize heat loss. The maximum outlet air temperature of 150°C was observed.

From the above literature review, it can be seen that there are many measures to enhance the performance of the parabolic trough solar collector. The present study proposes a triple-pass parabolic trough solar collector configuration so that the heat transfer fluid receives heat from the glass cover and absorber tube surfaces. Thus, the surface temperatures can be reduced leading to increase the collector efficiency. The independent parameters consist of tube diameters, collector length and Reynolds number of the heat transfer fluid to deduce heat transfer characteristics.

2. One-dimensional modeling

Figure 3 shows the schematic diagram of the triple-pass receiver. The receiver consists of an outer glass tube, an inner glass tube and an absorber. The tubes are fitted concentrically to each other so that the airflow moves in the three spaces. Air travels from the outermost annular space followed by the inner annular space and the inside of the absorber tube. **Figure 4** displays a diagram of thermal energy transfer between surfaces and the airflow and a thermal resistance circuit in which the heat conduction resistance of the tubes is neglected. The receiver collects solar radiation from the top half and concentrated radiation from the bottom half. The thermal balance for the glass tube 1 is written as Eq. (1). The solar thermal energy absorbed by the glass is equal to the heat transferred by radiation and convection to

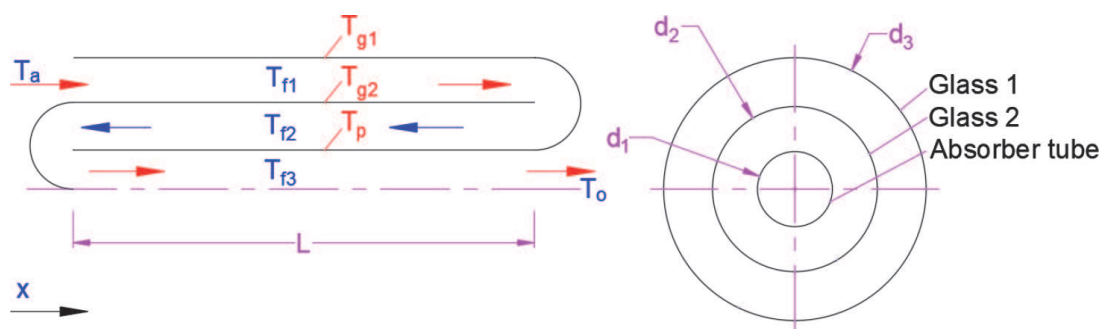


Figure 3.
 Details of receiver with triple pass airflow.

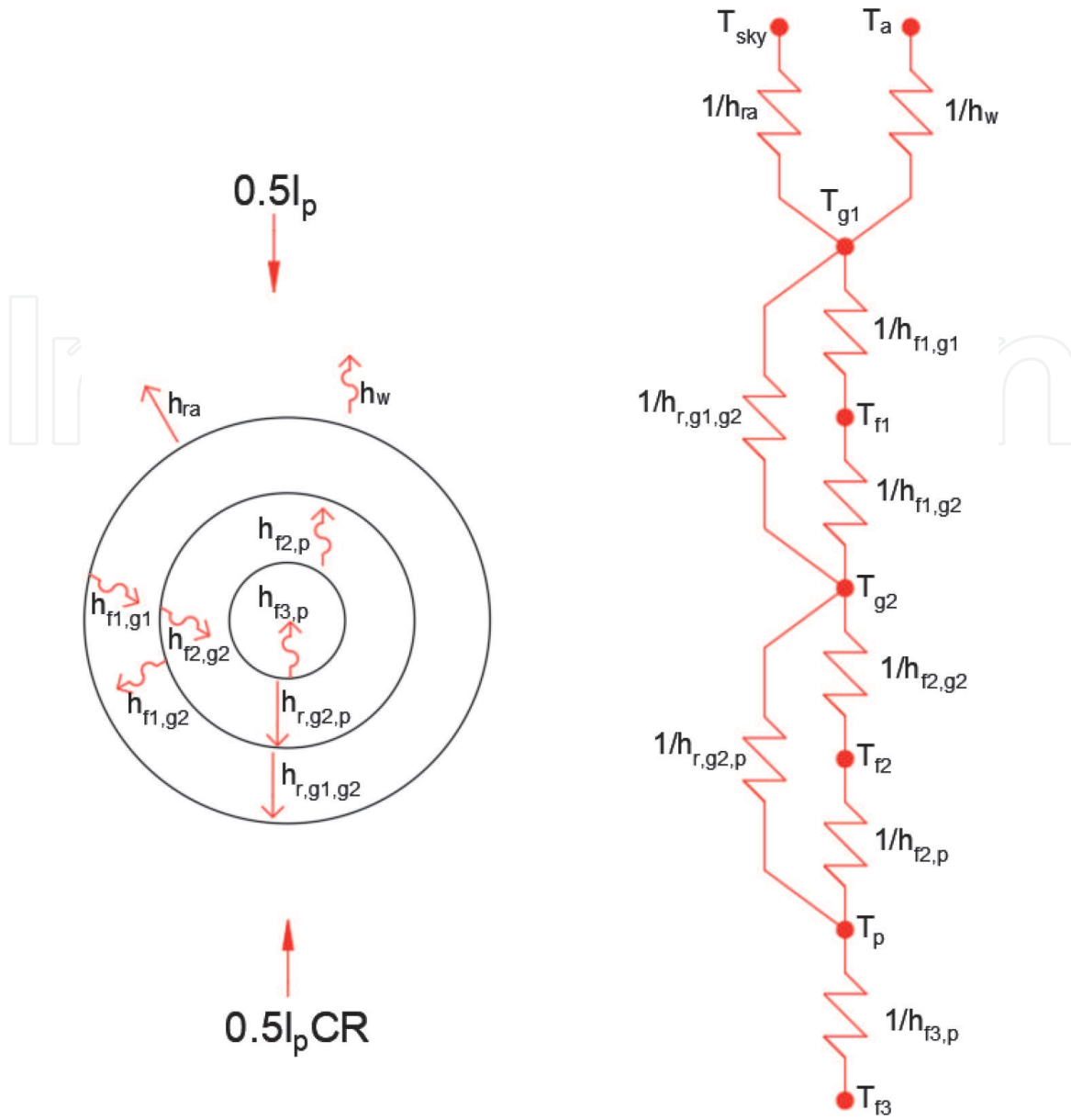


Figure 4. Energy balance diagram and thermal circuit of triple-pass parabolic trough solar air collector.

the environment, the heat transferred by convection to the fluid in the outer annulus (first pass), and the heat transferred by radiation to the glass tube 2 [6]:

$$I\alpha_{g1}A_{s1} + h_w A_{s3}(T_a - T_{g1}) + h_{ra} A_{s3}(T_{sky} - T_{g1}) + h_{r,g1,g2} A_{s2}(T_{g2} - T_{g1}) + h_{f1,g1} A_{s3}(T_{f1} - T_{g1}) = 0 \quad (1)$$

where I is solar radiation absorbed by the receiver and A_s is surface area of a tube. Solar radiation absorbed by the receiver is the sum of heat flux up and heat flux down [12]:

$$I = (0.5 + 0.5CR)I_p \quad (2)$$

The surface areas can be determined as:

$$A_{s1} = \pi d_1 L \quad (3)$$

$$A_{s2} = \pi d_2 L \quad (4)$$

$$A_{s3} = \pi d_3 L \quad (5)$$

T_{sky} is the sky temperature. $T_{sky} = 0.0552T_a^{1.5}$ [6].

CR and I_p in Eq. (2) are respectively the concentration ratio and solar radiation per unit area of a surface. CR is defined as [11]:

$$CR = \frac{A_{aperture}}{A_{s1}} \quad (6)$$

where $A_{aperture}$ is aperture area of the parabolic trough.

The temperature variation of the air along the axial direction in the first pass is due to convective heat exchange with the glasses 1 and 2:

$$\frac{dT_{f1}}{dx} = \frac{\pi d_3 h_{f1,g1}(T_{g1} - T_{f1}) + \pi d_2 h_{f1,g2}(T_{g2} - T_{f1})}{\dot{m}c_p} \quad (7)$$

Similar to the glass tube 1, heat exchange of the glass tube 2 is written as:

$$I\tau_{g1}\alpha_{g2}A_{s1} + h_{f1,g2}A_{s2}(T_{f1} - T_{g2}) + h_{f2,g2}A_{s2}(T_{f2} - T_{g2}) + h_{r,g1,g2}A_{s2}(T_{g1} - T_{g2}) + h_{r,g2,p}A_{s1}(T_p - T_{g2}) = 0 \quad (8)$$

The temperature variation of the air in the second pass is given by:

$$\frac{dT_{f2}}{dx} = \frac{\pi d_2 h_{f2,g2}(T_{g2} - T_{f2}) + \pi d_1 h_{f2,p}(T_p - T_{f2})}{\dot{m}c_p} \quad (9)$$

Heat balance of the absorber tube is presented as:

$$I\tau_{g1}\tau_{g2}\alpha_p A_{s1} + h_{f2,p}A_{s1}(T_{f2} - T_p) + h_{r,g2,p}A_{s1}(T_{g2} - T_p) + h_{f3,p}A_{s1}(T_{f3} - T_p) = 0 \quad (10)$$

The temperature variation of the air in the third pass is owing to convection heat transfer with the absorber tube surface:

$$\frac{dT_{f3}}{dx} = \pi d_1 h_{f3,p} \frac{T_p - T_{f3}}{\dot{m}c_p} \quad (11)$$

Convection and radiation heat transfer coefficients in Eqs. (1), (7)–(11) are determined by the following correlations:

- Convection heat transfer coefficient due to wind [6]:

$$h_w = 4V_w^{0.58}d_3^{-0.42} \quad (12)$$

- Forced convection heat transfer coefficient of the airflow in three passes by Dittus-Boelter correlation [14]:

$$\begin{aligned} h_{f1,g1} &= 0.023 Re_1^{0.8} Pr^{0.4} k / D_{e1} \\ h_{f1,g2} &= h_{f1,g1} \\ h_{f2,g2} &= 0.023 Re_2^{0.8} Pr^{0.4} k / D_{e2} \\ h_{f2,p} &= h_{f2,g2} \\ h_{f3,p} &= 0.023 Re^{0.8} Pr^{0.4} k / d_1 \end{aligned} \quad (13)$$

where Re_1 , Re_2 and Re are respectively Reynolds number in passes 1, 2, and 3. Pr is Prandtl number.

$$Re_1 = \rho D_{e1} V_1 / \mu \quad (14)$$

$$Re_2 = \rho D_{e2} V_2 / \mu \quad (15)$$

$$Re = \rho d_1 V_3 / \mu \quad (16)$$

In the above equations, D_e is the equivalent diameter of an annulus. The diameter can be estimated by:

$$D_{e1} = d_3 - d_2 \quad (17)$$

$$D_{e2} = d_2 - d_1 \quad (18)$$

- Radiation heat transfer coefficient of the outer glass to the sky [15]:

$$h_{ra} = \sigma \epsilon_{g1} (T_{g1}^2 + T_{sky}^2) (T_{g1} + T_{sky}) \quad (19)$$

- Radiation heat transfer coefficient of two glass tubes [4]:

$$h_{r,g1,g2} = \sigma (T_{g1}^2 + T_{g2}^2) \frac{T_{g1} + T_{g2}}{1/\epsilon_{g2} + (1 - \epsilon_{g1}) \frac{A_{s2}/A_{s3}}{\epsilon_{g1}}} \quad (20)$$

- Radiation heat transfer coefficient of the inner glass tube and the absorber tube [4]:

$$h_{r,g2,p} = \sigma (T_{g2}^2 + T_p^2) \frac{T_{g2} + T_p}{1/\epsilon_p + (1 - \epsilon_{g2}) \frac{A_{s1}/A_{s2}}{\epsilon_{g2}}} \quad (21)$$

- Air velocities in passes (V_1 , V_2 , and V_3) can be evaluated by mass conservation as:

$$\dot{m} = \left(\pi \frac{d_3^2}{4} - \pi \frac{d_2^2}{4} \right) \rho V_1 = \left(\pi \frac{d_2^2}{4} - \pi \frac{d_1^2}{4} \right) \rho V_2 = \pi \frac{d_1^2}{4} \rho V_3 \quad (22)$$

The energy amount of air received when passing through the receiver is determined as follows:

$$Q = \dot{m} c_p (T_o - T_a) \quad (23)$$

As the flow rate and receiver size change, the pumping power will also change to transport the fluid. The useful hydraulic energy of the air received from a blower is calculated as follows:

$$P_{flow} = \dot{m} \frac{\Delta P}{\rho} \quad (24)$$

where ΔP is the pressure difference of the air across the receiver. Because of significant length of the receiver, minor losses are omitted. The pressure drop due to friction in three 3 passes can be computed as:

$$\Delta P = \rho f_1 V_1^2 L / D_{e1} + \rho f_2 V_2^2 L / D_{e2} + \rho f_3 V_3^2 L / d_1 \quad (25)$$

where f is the friction factor of the air with the tube surface. The factor is calculated from the Blasius equation as follows [15]:

$$\begin{aligned} f_1 &= 0.059 Re_1^{-0.2} \\ f_2 &= 0.059 Re_2^{-0.2} \\ f_3 &= 0.059 Re^{-0.2} \end{aligned} \quad (26)$$

The effective efficiency of a parabolic trough collector taking into account the heat received, the power dissipated relative to the radiation absorbed by the receiver is calculated as follows:

$$\eta_{eff} = \frac{Q - P_{flow} / C_o}{A_s I} \quad (27)$$

where C_o is thermal energy conversion factor, $C_o = 0.2$ [16].

In this study, the absorber tube diameter was fixed. The diameter of the glass tubes, the Reynolds number of the air in the absorber tube, and the receiver length varied to investigate the axial temperature distribution and the collector efficiency. The diameters of the glasses change according to the diameter ratios which are defined as follows:

$$r_{23} = d_3 / d_2 \quad (28)$$

$$r_{12} = d_2 / d_1 \quad (29)$$

Table 1 presents the parameters entered into the mathematical model. The thermophysical parameters of the air (specific heat c_p , thermal conductivity k , density ρ , and dynamic viscosity μ) are estimated at the ambient temperature. Temperature variations of three surfaces and air in three passes can be solved by numerical integrals of temperature gradient equations, i.e., Eqs. (7), (9), and (11). The one-dimensional (1D) computational domain along the tube is divided into control volumes corresponding to a spatial step Δx . Solving the ordinary differential equations can be utilized ode45 function in MATLAB software [17] or integral function in EES software [18]. **Figure 5** presents a comparison of the air flow

Parameter	Value
Concentration ratio	CR = 10
Solar radiation	$I_p = 848 \text{ W/m}^2$
Ambient temperature	$T_a = 27^\circ\text{C}$
Absorptivity of glass covers	$\alpha_{g1} = \alpha_{g2} = 0.05$
Absorptivity of absorber tube	$\alpha_p = 0.92$
Emissivity of glass covers	$\epsilon_{g1} = \epsilon_{g2} = 0.92$
Emissivity of absorber tube	$\epsilon_p = 0.92$
Transmissivity of glass cover	$\tau_{g1} = \tau_{g2} = 0.84$
Wind velocity	$V_w = 1 \text{ m/s}$
Absorber tube diameter	$d_1 = 42 \text{ mm}$

Table 1.
 Input parameters.

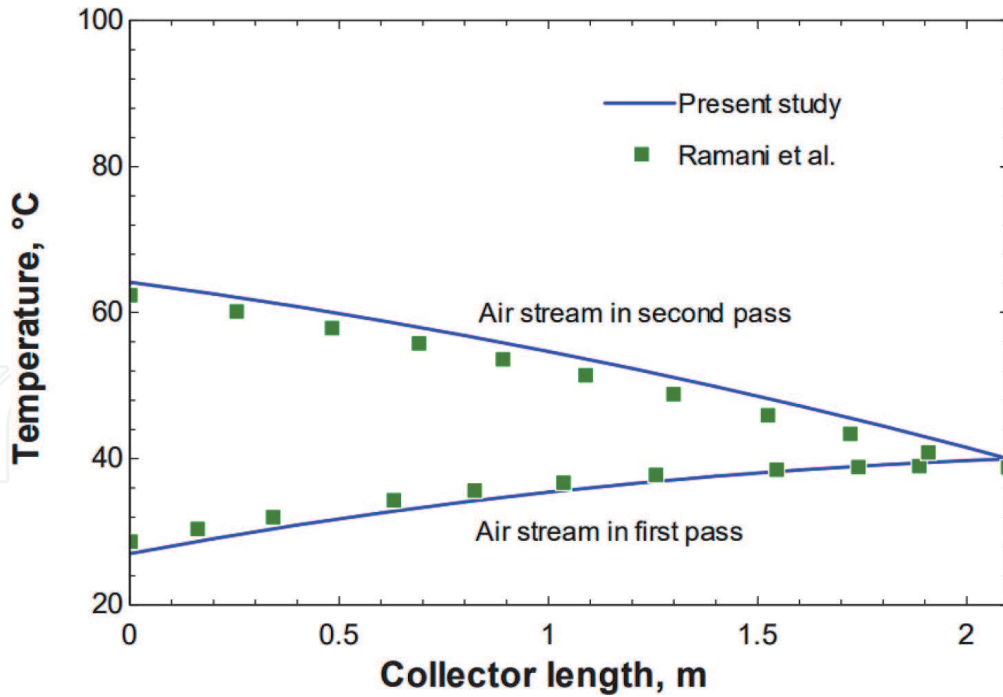


Figure 5. Confirmation of air temperature along the collector length with published data [19].

temperature variation in a double-pass solar air heater between the results from the code developed in this study and those of the literature [19]. It can be seen that the two results are close to each other and the difference is not significant. Therefore, the model formulation in this study is accuracy to perform the parametric study for the triple pass parabolic trough solar air collector.

3. Results and discussion

This section investigates the influence of Reynolds number in the range 10000 to 16000, tube diameter ratios (r_{23} and r_{12}) from 1.2 to 2, and tube length from 1.5 to 3.5 m on the collector efficiency and temperature distribution of the receiver.

Figure 6 shows the effect of Re and r_{23} on the performance. It can be seen that when the Re number increases, the performance increases. For flat-plate air collectors, efficiency can peak at some Re. However, for a concentrating collector, the thermal duty is very large compared to pumping power. Therefore, when Re increases, the heat transfer rate increases more than increase in the pressure loss penalty. However, the efficiency increases slightly with the Re number because the pumping power increases significantly with the flow rate. At fixed Re, the performance peaks at certain r_{23} . As the ratio increases, the diameter of the glass covers increases, which reduces the heat transfer rate due to the decrease in air velocity. Conversely, increasing this ratio reduces the pressure loss in the two annuli. This trade-off leads to the optimal r_{23} . **Figure 6** shows that the optimal r_{23} value is almost unchanged with Re, i.e., $r_{23, \text{opt}} = 1.55$. **Figure 7** presents the effect of the ratio of inner glass tube diameter to absorber tube diameter on the efficiency. The effect of r_{12} can be seen to be more pronounced than that of r_{23} . This is attributed to mainly heat exchange in the second pass due to the high temperatures of the absorber tube and glass 2. The optimum r_{12} varies over a wider range from 1.45 to 1.5. Also, at certain Re number, the performance changes drastically with r_{12} , especially at large Re numbers. At Re = 16000, the efficiency varies from 0.59 to 0.6 with r_{23} , from 0.575 to 0.605 with r_{12} .

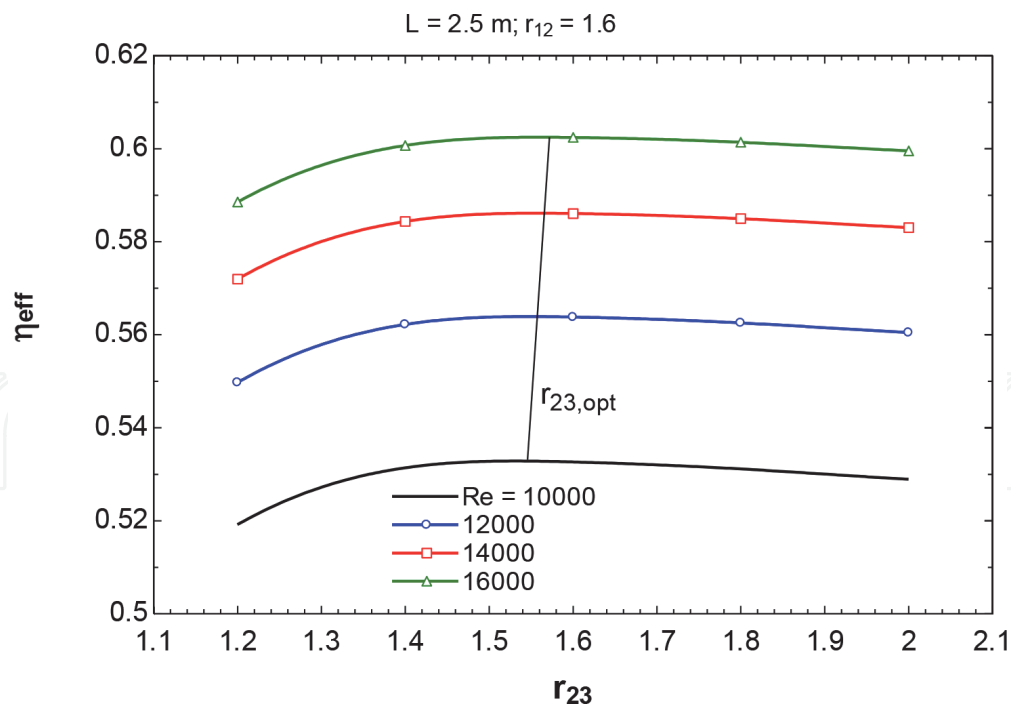


Figure 6.
 Effect of Reynolds number and diameter ratio of glasses.

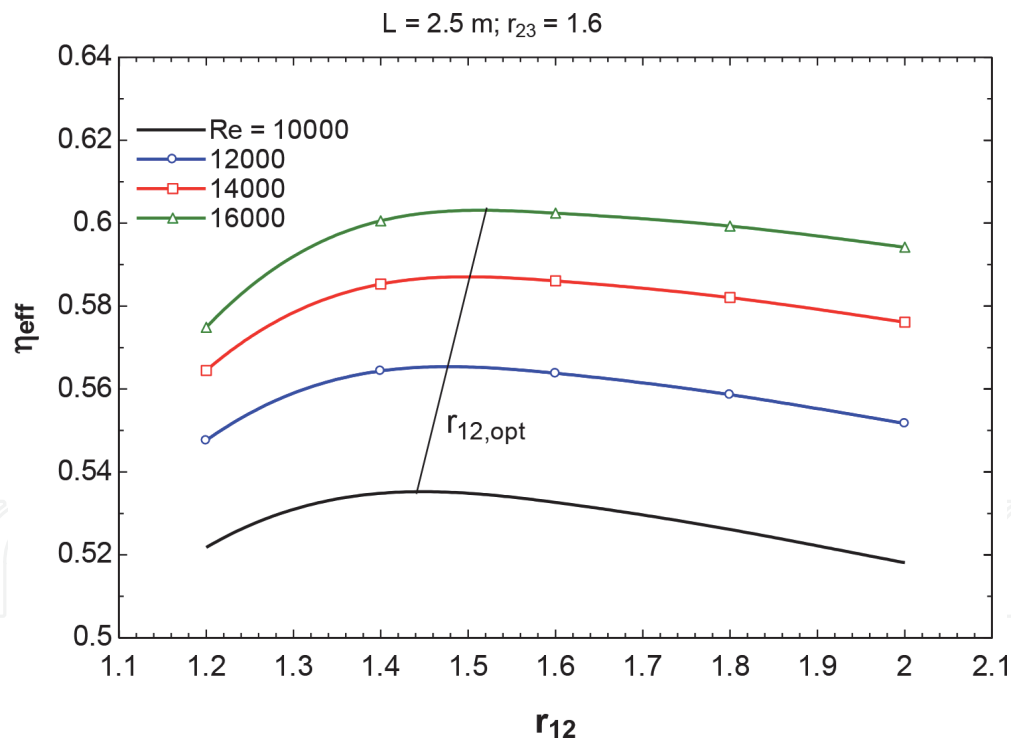


Figure 7.
 Effect of Reynolds number and diameter ratio of glass 2 and absorber tube.

Figure 8 depicts the effect of collector length (L) on collector efficiency. It is observed that as the length increases, the efficiency decreases. It is noted that for a concentrating collector, the thermal power is very large compared to the pumping power. Therefore, the optimum L and Re are not found to maximize the efficiency as can be observed in flat-plate solar collectors. As the length increases, at a certain pass, the air temperature increases, reducing the temperature difference between the heat exchanger surfaces and the air temperature. This small temperature

difference causes poor heat transfer rate. The reduction in efficiency with the length in the concentrator is also similar to that of the flat plate collector [15].

Figures 9 and **10** illustrate the distributions of the six temperatures along the tube length at $Re = 10000$. **Figure 9** plots the temperatures at the optimal diameter ratios for this Re , i.e., $r_{12} = 1.44$ and $r_{23} = 1.56$. While **Figure 10** represents worst-case temperatures ($r_{12} = 2$ and $r_{23} = 1.2$) for the sake of comparison. It is clear that the average temperature of the absorber tube decreases markedly from 160°C (the worst case) to 145°C (the optimum case). This reveals the optimal case owning better heat exchange of the fluid in passes 2 and 3 with absorber tube surface and

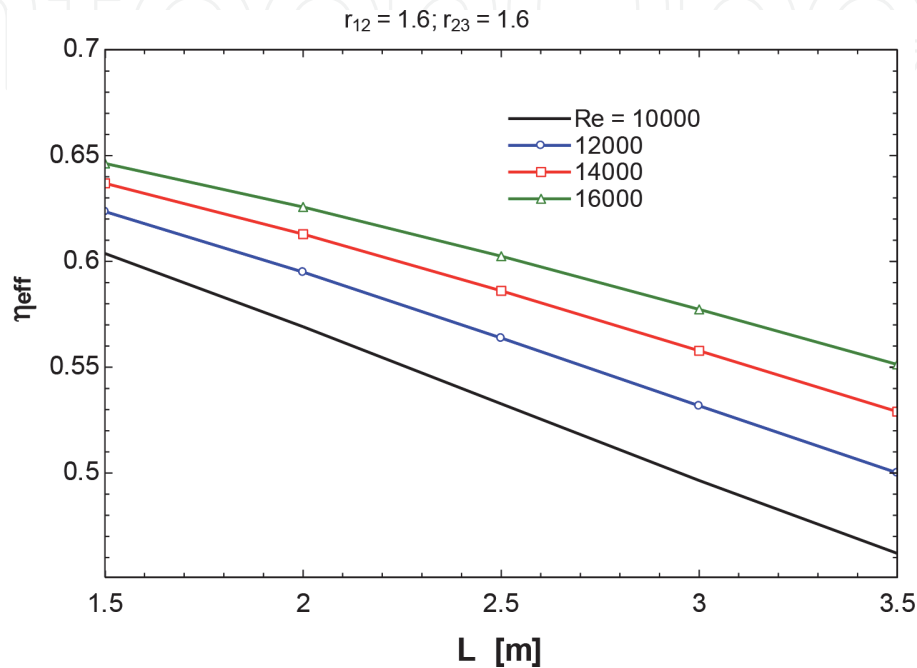


Figure 8.
Effect of Reynolds number and collector length.

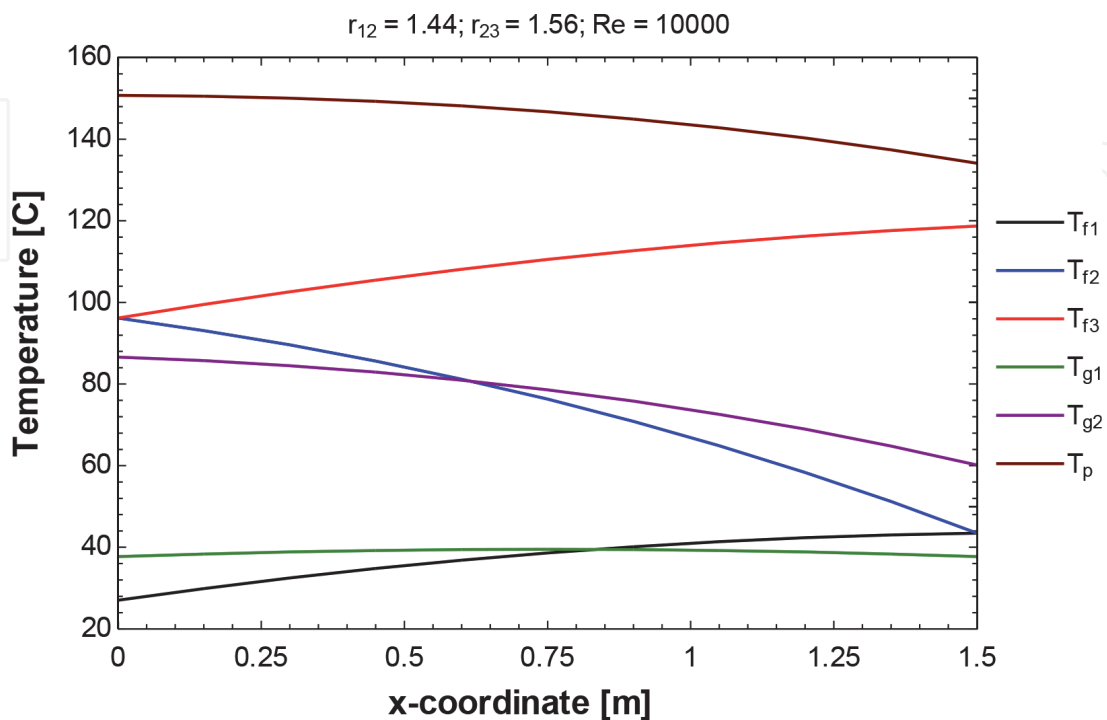


Figure 9.
Local temperature distribution of the airflow in passes and surfaces at optimum ratios.

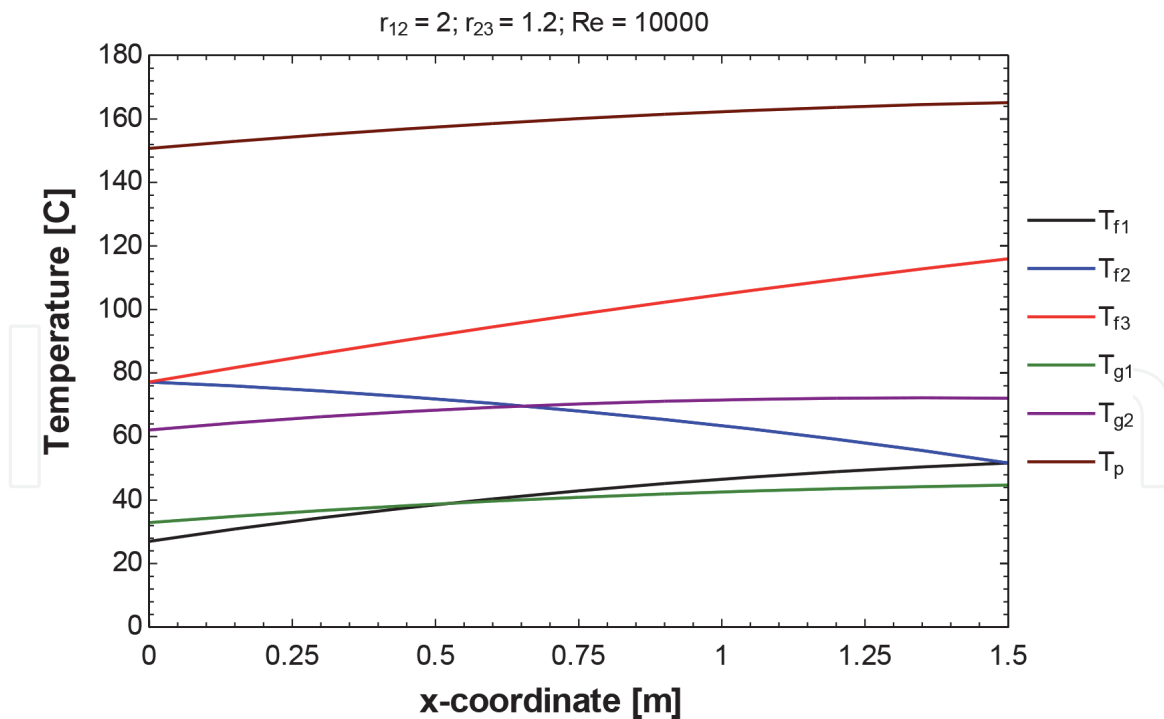


Figure 10.
 Local temperature distribution of the airflow in passes and surfaces at the worst ratios.

smaller heat loss. For the optimal case, the absorber tube temperature increases with the air temperature in the second pass. In contrast, the absorber tube temperature increases with the air temperature in third pass for the worst case. Furthermore, the temperature cross between the air in pass 1 and glass 1 occurs in the very short segment from the inlet in the worst case. The temperature differences in pass 2 of **Figures 9** and **10** are 55 K and 28 K, respectively. From **Figures 9** and **10** it can be recognized that there are two temperature crosses between T_{f1} and T_{g1} , and between T_{f2} and T_{g2} . If shorter tubes are used, a temperature cross may not occur. Therefore, it can be concluded that collector efficiency decreases with increasing tube length by means of the current axial temperature analysis.

4. Conclusions

A 1D analytical model has been presented in this chapter to predict the local temperature of fluid and heat exchanger surfaces of the triple-pass parabolic trough solar collector. Some important conclusions are drawn as follows:

- The diameter ratios of outer to inner glasses of 1.55 and the inner glass to absorber tube in the range of 1.45 to 1.5 achieve the greatest effective efficiency.
- The efficiency increases with Reynolds number and decreases with tube length. In other words, optimum Reynolds number and tube length were not found due to the fact that thermal power prevails over pumping power for a concentrating solar collector.
- The absorber tube temperature is reduced up to 15 K with optimal diameter ratios.
- The effect of r_{12} on efficiency is more significant than that of r_{23} due to the strong heat exchange of the airflow in the annular space between the absorber tube and the inner glass tube.

Acknowledgements

This research is funded by the Vietnam National University-Ho Chi Minh City (VNU-HCM) under grant number B2021-20-06.

Conflict of interest

The authors declare no conflict of interest.

Author details

Nguyen Minh Phu^{1*} and Ngo Thien Tu^{2,3}

1 Faculty of Heat and Refrigeration Engineering, Industrial University of Ho Chi Minh City (IUH), Ho Chi Minh City, Vietnam

2 Faculty of Mechanical Engineering, Ho Chi Minh City University of Technology (HCMUT), Ho Chi Minh City, Vietnam

3 Viet Nam National University, Ho Chi Minh City, Vietnam

*Address all correspondence to: nguyenminhphu@iuh.edu.vn

IntechOpen

© 2021 The Author(s). Licensee IntechOpen. This chapter is distributed under the terms of the Creative Commons Attribution License (<http://creativecommons.org/licenses/by/3.0>), which permits unrestricted use, distribution, and reproduction in any medium, provided the original work is properly cited. 

References

- [1] Phu NM, Luan NT. A Review of Energy and Exergy Analyses of a Roughened Solar Air Heater. *Journal of Advanced Research in Fluid Mechanics and Thermal Sciences*. 2020;77(2): 160-175.
- [2] Phu NM, Hap NV. Performance Evaluation of a Solar Air Heater Roughened with Conic-Curve Profile Ribs Based on Efficiencies and Entropy Generation. *Arabian Journal for Science and Engineering*. 2020;45(11):9023–9035.
- [3] Phu NM, Hung HN, Tu NT, Van Hap N. Analytical predictions of exergoeconomic performance of a solar air heater with surface roughness of metal waste. *Journal of Thermal Analysis & Calorimetry*. 2021;144(5).
- [4] Elakhdar M, Landoulsi H, Tashtoush B, Nehdi E, Kairouani L. A combined thermal system of ejector refrigeration and Organic Rankine cycles for power generation using a solar parabolic trough. *Energy Conversion and Management*. 2019;199:111947.
- [5] Li T, Yuan C. An optimal design analysis of a novel parabolic trough lighting and thermal system. *International Journal Of Energy Research*. 2016;40(9):1193-1206.
- [6] Bozorg MV, Doranehgard MH, Hong K, Xiong Q. CFD study of heat transfer and fluid flow in a parabolic trough solar receiver with internal annular porous structure and synthetic oil–Al₂O₃ nanofluid. *Renewable Energy*. 2020;145:2598-2614.
- [7] Bellos E, Tzivanidis C, Belessiotis V. Daily performance of parabolic trough solar collectors. *Solar Energy*. 2017;158: 663-678.
- [8] Okonkwo EC, Abid M, Ratlamwala TA. Effects of synthetic oil nanofluids and absorber geometries on the exergetic performance of the parabolic trough collector. *International Journal of Energy Research*. 2018;42(11):3559-3574.
- [9] Kaloudis E, Papanicolaou E, Belessiotis V. Numerical simulations of a parabolic trough solar collector with nanofluid using a two-phase model. *Renewable Energy*. 2016;97:218-229.
- [10] Ray S, Tripathy AK, Sahoo SS, Bindra H. Performance analysis of receiver of parabolic trough solar collector: Effect of selective coating, vacuum and semitransparent glass cover. *International Journal of Energy Research*. 2018;42(13):4235-4249.
- [11] Tzivanidis C, Bellos E. The use of parabolic trough collectors for solar cooling—A case study for Athens climate. *Case Studies in Thermal Engineering*. 2016;8:403-413.
- [12] Ghasemi SE, Ranjbar A. Effect of nanoparticles in working fluid on thermal performance of solar parabolic trough collector. *Journal of Molecular Liquids*. 2016;222:156-166.
- [13] Nain S, Parinam A, Kajal S. Experimental study and analysis of air heating system using a parabolic trough solar collector. *International Journal of Ambient Energy*. 2018;39(2):143-146.
- [14] Thao PB, Truyen DC, Phu NM. CFD Analysis and Taguchi-Based Optimization of the Thermohydraulic Performance of a Solar Air Heater Duct Baffled on a Back Plate. *Applied Sciences*. 2021;11(10):4645.
- [15] Nguyen Thanh L, Nguyen Minh P. First and Second Law Evaluation of Multipass Flat-Plate Solar Air Collector and Optimization Using Preference Selection Index Method. *Mathematical Problems in Engineering*. 2021;2021: 5563882.

[16] Matheswaran M, Arjunan T, Somasundaram D. Energetic, exergetic and enviro-economic analysis of parallel pass jet plate solar air heater with artificial roughness. *Journal of Thermal Analysis and Calorimetry*. 2019;136(1): 5-19.

[17] Phu NM, Lee GS. Characteristics of pressure and force considering friction in a closed cylinder with a holed piston. *Journal of Mechanical Science and Technology*. 2014;28(6):2409-2415.

[18] Phu NM. A compact EES program to predict the axial temperature distribution in triple-fluid heat exchanger. *Science & Technology Development Journal*. 2020;3(3): 452-460.

[19] Ramani B, Gupta A, Kumar R. Performance of a double pass solar air collector. *Solar energy*. 2010;84(11): 1929-1937.

IntechOpen